

# Field dependence of the $\text{Eu}^{2+}$ spin relaxation in $\text{EuFe}_{2-x}\text{Co}_x\text{As}_2$

F.A. Garcia, A. Leithe-Jasper, W. Schnelle, M. Nicklas, H. Rosner, and J. Sichelschmidt

Max Planck Institute for Chemical Physics of Solids, 01187 Dresden, Germany

**Abstract.** The layered compound  $\text{EuFe}_2\text{As}_2$  is an interesting model system to investigate the effects of well defined local  $\text{Eu}^{2+}$   $4f$  states on the itinerant electronic and magnetic properties of the FeAs layers. To address this subject, we investigated the series  $\text{EuFe}_{2-x}\text{Co}_x\text{As}_2$  ( $0.1 \leq x \leq 0.75$ ) by electron spin resonance (ESR) of  $\text{Eu}^{2+}$  to probe the spin dynamics of the itinerant subsystem. We relate the results to dc-susceptibility measurements and band structure calculations. As a consequence of the weak coupling between the local and itinerant subsystems we found that the spin relaxation is well understood in terms of the exchange coupling among the local  $\text{Eu}^{2+}$  spins. A pronounced field dependence of the  $\text{Eu}^{2+}$  spin relaxation demonstrates the direct influence of magnetic fluctuations at the  $\text{Fe}_{2-x}\text{Co}_x\text{As}_2$  layers.

## 1. Introduction

The discovery of superconductivity in iron-based pnictides [1, 2] sparked a tremendous surge of interest and research activities. This class of materials displays a high structural and chemical flexibility comprising several closely related structure types based on common layered Fe-pnictogen building blocks. Depending on charge-carrier doping, external or chemical pressure they all show a subtle interplay among structural transitions, antiferromagnetism (AFM) and superconductivity [3]. The relevance of magnetic fluctuations for the stabilization of the superconducting state has been put forward for unconventional superconductors which are found among a wide range of compound families [4, 5, 6]. Their role in superconducting iron-pnictides are now subjected to intense scrutiny. In this context, the compound  $\text{EuFe}_2\text{As}_2$  (with the body centered tetragonal  $\text{ThCr}_2\text{Si}_2$ - type of structure, where layers of  $\text{Fe}_2\text{As}_2$  alternate with Eu layers along the  $c$ -axis) was presented as an important model system to study the interplay between well defined  $4f$  magnetic states and the electronic properties of the iron-arsenide layer [7, 8, 9].

$\text{EuFe}_2\text{As}_2$  is an intermetallic compound which undergoes both a spin density wave (SDW) type antiferromagnetic phase transition at  $T_N^{\text{SDW}} = 195$  K, associated with the itinerant states of the FeAs subsystem, and a localized AFM ordering taking place at  $T_N^{\text{Eu}} = 22$  K, associated with the Eu  $4f$  local moments subsystem [7, 8]. The magnetic structure of the local moment subsystem consists of  $\text{Eu}^{2+}$  layers in a ferromagnetic order, stacked antiferromagnetically along the  $c$ -axis [10]. It has been shown that upon substitution on any of the Eu (K substitution) [11], Fe (Co substitution) [12] and As (P substitution) sites [13, 14], the itinerant AFM state is suppressed and the onset of a superconducting phase is observed. Similar behavior is also found when the host compound is subjected to external pressure, that is also claimed to lead to the appearance of reentrant superconductivity [15, 16].

Notwithstanding the large effects observed in the itinerant AFM phase, the energy scale of the local moment interaction, as compared to the energy scale of the itinerant subsystem, has been observed to be only slightly modified in all of these substitutional studies. This suggests a weak coupling between the local  $4f$  electronic states and the electronic and magnetic properties of the FeAs layers. Further indication in this direction is also drawn from the study of the rather weak suppression of the superconducting state by the inclusion of Eu in optimally doped  $\text{Sr}_{1-y}\text{Eu}_y\text{Fe}_{2-x}\text{Co}_x\text{As}_2$  [17], from the lack of signatures on the electronic structure of  $\text{EuFe}_2\text{As}_2$  when the  $\text{Eu}^{2+}$  subsystem undergoes the AFM transition [18] and from magnetotransport studies [19].

The nature of the local moment ordering, however, is changed from AFM to ferromagnetic (FM) upon substitution of As by P [13] and possibly also for Fe by Co [20]. In the case of P substitution, it seems clear that the change from AFM to FM order is related to both structural effects and substitutional effects [13]. This is in contrast to the Co substitution, where the change in the electron filling is supposed to be the dominant effect, allowing a more controlled investigation.

In searching a comprehensive description of the magnetic and electronic properties of the FeAs layers, the electron spin resonance of  $\text{Eu}^{2+}$  has proven to be a suitable tool to provide information on the spin dynamics in  $\text{EuFe}_2\text{As}_2$  [21]. In this respect, a proper understanding of the  $\text{Eu}^{2+}$  spin relaxation is essential, and especially needs to be considered for *concentrated*  $\text{Eu}^{2+}$  ions like in  $\text{EuFe}_{2-x}\text{Co}_x\text{As}_2$ . In case of  $\text{Eu}^{2+}$  ions *diluted* in a metallic environment, the spin relaxation is determined by the exchange scattering between the local and itinerant spins (the Korringa process) and should be sensitive to the spin dynamics of both [22]. However, in concentrated magnetic compounds, the electronic spin relaxation is expected to be determined more by the exchange coupling among the local spins [23, 24] which is sensitive to an externally applied magnetic field. Therefore, a systematic investigation of the field dependence of the ESR in  $\text{EuFe}_{2-x}\text{Co}_x\text{As}_2$  and an interpretation in terms of concentrated  $\text{Eu}^{2+}$  ions provide a unique tool to evaluate the relation between the local moment magnetism and the magnetic and electronic properties of the itinerant subsystem.

To this aim, along with dc-susceptibility measurements, we present the  $\text{Eu}^{2+}$  ESR at three different magnetic fields, corresponding to resonance frequencies of 1.1 GHz (*L*-band), 9.4 GHz (*X*-band) and 34 GHz (*Q*-band). We shall discuss a significant reinterpretation of the available ESR data [21, 25, 12, 26], that do not include an investigation on the field dependence of the relaxation. The field dependence of the relaxation is a strong piece of evidence that the Eu *4f* local moments are coupled with the  $\text{Fe}_{2-x}\text{Co}_x\text{As}_2$  itinerant magnetic fluctuations. Furthermore, we have also performed band structure calculations to guide our discussion on the nature of the  $\text{Eu}^{2+}$  spin relaxation.

The local moment relaxation is sensitive to the exchange coupling between the local spins by virtue of the so-called bottleneck effect [22]. It occurs when the conduction electron-lattice scattering rate ( $1/T_{\text{ceL}}$ ) is smaller than, or comparable to, the conduction electron-magnetic ion ( $1/T_{\text{ceI}}$ ) scattering rate. In this situation, after being scattered by the magnetic center (the Korringa process), the conduction electrons, instead of dissipating energy to the lattice, give this energy back to the magnetic ion system (Overhauser process). As a consequence, one may probe a suppressed Korringa process [22, 27, 28], since the slow  $1/T_{\text{ceL}}$  will modulate the Korringa rate. However, it may also occur that the relaxation simply does not reflect the exchange scattering between the local moments and the conduction electrons, being determined primarily by the exchange coupling between the  $\text{Eu}^{2+}$  ions [23, 24].

Even in the latter scenario the properties of the  $\text{Fe}_{2-x}\text{Co}_x\text{As}_2$  itinerant subsystem can be deduced from the local moment relaxation, since the coupling among local spins is realized through the Ruderman-Kittel-Kasuya-Yosida (RKKY) indirect exchange interaction. Hence, while mediating the exchange coupling of the local subsystem, the itinerant subsystem manifest its properties in the local moment relaxation. This interplay qualifies the  $\text{Eu}^{2+}$  ESR as a suitable probe for the spin dynamics taking place in the  $\text{Fe}_{2-x}\text{Co}_x\text{As}_2$  layers.

## 2. Methods

Details of the synthesis of polycrystalline samples of  $\text{EuFe}_{2-x}\text{Co}_x\text{As}_2$  ( $0.1 \leq x \leq 0.75$ ) are given in Ref. [20]. The actual content of Co was determined by energy dispersive X-ray scattering (EDX) and are very close to the nominal values. The physical properties of the samples used in this experiment are presented in Ref. [20]. The ESR measurements were carried out using a Bruker Elexsys 500 spectrometer for  $L$ -band (1.1 GHz),  $X$ -band (9.4 GHz) and  $Q$ -band (34 GHz) frequencies in the temperature intervals  $30 \leq T \leq 120$  K for the  $L$ -band and  $4.2 \leq T \leq 300$  K for both  $X$ -band and  $Q$ -band measurements.

The samples used in the ESR measurements were sieved in a fine powder to achieve grain size homogeneity. In the whole temperature interval, the spectrum consisted of an asymmetric exchange narrowed single broad line. The ESR parameters were obtained through the fitting of the observed spectra according the formula given in Refs. [29, 30] which takes also the effect of a counter resonance in broad ESR lines into account. The parameters included in the fitting are the ESR linewidth  $\Delta H$ , the resonance field  $H_{\text{res}}$ , the spectrum amplitude and the lineshape parameter  $\alpha = D/A$ , which takes into account the dispersion to absorption ratio of the microwave radiation when it probes a metallic surface ( $D = 0$  in insulators). In the whole temperature interval, the best fitting was always given by this procedure, although we have also tried to search for contributions given by unresolved crystal field (CF) effects and other magnetic anisotropy effects which could be present in the powder spectra. The dc-susceptibility of the samples was measured using a commercial MPMS SQUID dc magnetometer (Quantum Design).

Scalar-relativistic density functional (DFT) electronic structure calculations were performed using the full-potential FPLO code [31], version fpl9.01-35. For the exchange-correlation potential, within the local density approximation (LDA) the parametrization of Perdew-Wang [32] was chosen. To obtain precise band structure information, the calculations were carried out on a well converged mesh of 4096  $k$ -points (16x16x16 mesh, 405 points in the irreducible wedge of the Brillouin zone). The partial Fe substitution with Co was modeled within the virtual crystal approximation (VCA) as implemented according to Ref. [33]. Since the structural changes upon partial Co substitution are small in the investigated concentration range, the experimental structural data for the undoped tetragonal  $\text{EuFe}_2\text{As}_2$  compound (space group  $I4/mmm$ ,  $a = 3.916\text{\AA}$ ,  $c = 12.052\text{\AA}$  and  $z_{\text{As}} = 0.3625$ ) [34] were used throughout the calculations. The strong Coulomb repulsion for the Eu  $4f$  states were treated within the LSDA+ $U$  approximation with  $U = 8$  eV as a typical value for Eu. The resulting density of states (DOS) is essentially unchanged for a variation of  $U$  within the physically relevant range.

## 3. Results and Discussion

In Fig. 1(a) we present the temperature ( $T$ ) vs. Co-content ( $x$ ) phase diagram for the series  $\text{EuFe}_{2-x}\text{Co}_x\text{As}_2$ , mostly based on our previous investigation [20]. The general

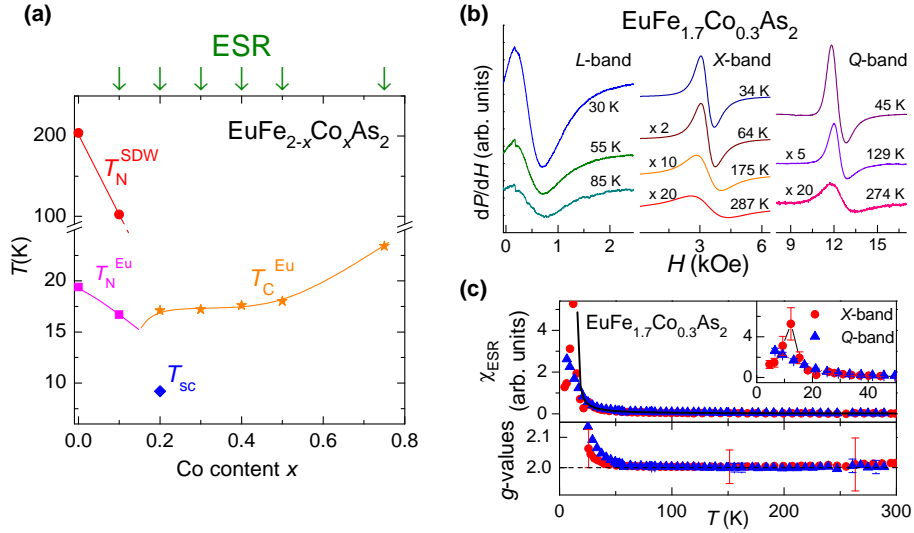


**Figure 1.** (Color online) General characteristics of the investigated samples. (a) Temperature ( $T$ ) vs  $x$  phase diagram for the  $\text{EuFe}_{2-x}\text{Co}_x\text{As}_2$  series. Arrows indicate the samples measured by ESR. (b) Survey of representative ESR spectra for  $x = 0.3$  taken at  $L$ -band (1.1 GHz),  $X$ -band (9.4 GHz), and  $Q$ -band (34 GHz). Magnifying factors are listed on the left side of the corresponding spectrum lines. (c) ESR intensity ( $\chi_{\text{ESR}}$ ) and ESR  $g$ -values measured at  $X$ - and  $Q$ -band for  $x = 0.3$ .  $\chi_{\text{ESR}}$  displays a Curie-like behavior (solid line) as expected for a local moment. The inset shows that at lower temperatures the evolution of  $\chi_{\text{ESR}}$  is frequency/field dependent. The ESR  $g$ -values assume a constant value of  $g = 2$  (dashed line) for  $T \geq 60$  K.

properties of our ESR investigation for the  $\text{EuFe}_{1.7}\text{Co}_{0.3}\text{As}_2$  sample are shown in Fig. 1(b) (representative ESR spectra) and in Fig. 1(c) [ESR intensity ( $\chi_{\text{ESR}}$ ),  $g$ -values]. The phase diagram shows that the SDW order, is fully suppressed for  $x = 0.2$ . This is also the only sample for which we could confirm a transition to a superconducting phase [see  $T_{\text{sc}}$  symbol in Fig 1(a)]. Furthermore, our magnetization measurements suggest that, for  $x \geq 0.2$ , the Eu local moment ordering changes from AFM to FM. These results are quite similar to those obtained by the substitution of As by P [13, 14], where superconductivity is found only in a narrow region of the phase diagram and the nature of the local order also changes on substitution. This similarity suggests that lattice structural effects, rather than the effects of electronic doping, play a fundamental role in tuning the phase diagram in these substitutional studies [35]. However, more detailed investigations are required since other works addressing the substitution of Fe by Co reported that a transition to a superconducting state is realized in a much broader interval of Co-substitution [12, 36].

Direct inspection of the ESR spectra in Fig. 1(b) reveal that the change in frequency corresponds to a change of the magnetic fields applied to the sample. We point out that according to the resonance condition  $\hbar\omega = g\mu_B H_{\text{res}}$  the typical fields, for  $g = 2.0$ , are roughly 340 Oe for  $L$ -band, 3400 Oe for  $X$ -band and 12000 Oe for  $Q$ -band. In addition, the  $L$ -band measurements are meaningful only in a relatively narrow

temperature interval ( $30 \leq T \leq 120$  K), since beyond this interval the broadening of the line makes the fitting process to be highly questionable. Furthermore, we will only discuss the  $L$ -band ESR linewidth ( $\Delta H$ ).

$\chi_{\text{ESR}}$  [Fig.1(c)] is given by the the double integration of the observed spectra. For  $T \geq 40$  K no differences between the  $X$ -band and  $Q$ -band results can be resolved. In this temperature region,  $\chi_{\text{ESR}}$  follows a Curie-Weiss like behavior, indicated by the solid line in the figure, as expected for well defined local moments. In the inset, we show the low temperature data. The peak observed in the  $X$ -band  $\chi_{\text{ESR}}$  marks the transition temperature of the local moment magnetic order ( $T_{\text{N}}^{\text{Eu}}$ ). This peak is not observed in the  $Q$ -band  $\chi_{\text{ESR}}$  (i.e. at higher fields), suggesting that the nature of the local moment magnetic ordering changes from AFM to FM. However, it is indicating that some field needs to be applied to fully stabilize the FM order in the region  $x \geq 0.2$  shown in the phase diagram.

The  $g$ -values [Fig. 1(c)] are obtained from the resonance condition. For  $T \geq 60$  K, they assume a constant value of  $g = 2$  that is close to the  $\text{Eu}^{2+}$  ionic value of  $g = 1.993$  found in insulators. At lower temperatures, the  $g$ -values increase due to the onset of the internal fields associated with the magnetic ordering of the local moments.

In metals, in the absence of a bottleneck effect, it is expected that the resonance position of a given paramagnetic ion is shifted with respect to its value in insulators [22]. This  $g$ -shift ( $\Delta g = g_{\text{exp}} - g_{\text{ins}}$ ) is given by

$$\Delta g = \langle \eta(E_F) J(q=0) \rangle_{Av} = \eta(E_F) \langle J(q=0) \rangle_{Av} \quad (1)$$

where in Eq. 1  $\langle J(q=0) \rangle_{Av}$  denotes an average over the Fermi surface of the  $q = 0$  component of the exchange interaction  $J(q)$ , between the local moment and the itinerant states, and  $\eta(E_F)$  is a constant DOS for a given spin direction at the Fermi surface (states  $\text{eV}^{-1}\text{mol}^{-1}\text{spin}^{-1}$ ). Therefore, one expects the  $g$ -values to reflect the evolution of the Fermi surface and magnetic properties of the  $\text{Fe}_{2-x}\text{Co}_x\text{As}_2$  layers, both supposed to be induced by Co-substitution. In contrast, the  $g$ -values show nearly the same behavior for all measured samples, indicating that they seem to reflect only the properties of the local moment. This is a feature expected to be found in systems in a strong bottleneck regime [22, 24].

Whereas the  $g$ -values usually reflect static properties, it is expected that  $\Delta H$  should be a direct probe of the dynamical behavior of the electronic spin. Experiments on  $\text{EuFe}_2\text{As}_2$  [21, 26] single crystals have revealed two distinct behaviors of  $\Delta H$ . On one hand, for  $T > T_{\text{N}}^{\text{SDW}}$ , a Korringa-like relaxation was found, meaning that  $\Delta H = \Delta H_0 + b_K T$ , where  $\Delta H_0$  is the residual linewidth ( $\Delta H$  at  $T = 0$ ) and  $b_K$  is the Korringa rate, which is determined by the exchange scattering of the local moments (the  $4f$   $\text{Eu}^{2+}$  localized states) by the itinerant electronic states (electronic states of  $\text{FeAs}$  layers). On the other hand, for  $T < T_{\text{N}}^{\text{SDW}}$ ,  $\Delta H$  was shown to display an angular dependence but was found to be nearly temperature independent. This was discussed in terms of a suppressed Korringa relaxation due to the gap opening at  $T_{\text{N}}^{\text{SDW}}$ .

These ideas were drawn on the basis that in metals, in the absence of a bottleneck, the Korringa rate is given by [22]:

$$\begin{aligned} b_K &= \frac{\pi k_B}{g\mu_B} \left\langle (N(E_F)J(k_F, k'_F))^2 \right\rangle_{Av} = \frac{\pi k_B}{g\mu_B} \eta(E_F)^2 \langle J(q)^2 \rangle_{Av} \\ &\equiv \frac{\pi k_B}{g\mu_B} \eta(E_F)^2 J^2 \end{aligned} \quad (2)$$

where  $k_B$  is Boltzmann constant,  $g$  is the measured  $g$ -value,  $\mu_B$  is the Bohr magneton, and  $\langle J(q)^2 \rangle_{Av} \equiv J^2$  is the average over the Fermi surface of the  $q$ -dependent exchange coupling  $J(q)$ . In this picture, the gap opening at  $T_N^{\text{SDW}}$  would make  $\eta(E_F)$  to vanish (or to decrease significantly), thus changing the relaxation regime. The evolution of  $\Delta H$  upon Co-substitution was also discussed in these terms, although details were not given [12].

The bottleneck effect does introduce an important modification in Eq. 2. In the bottleneck regime, the apparent Korringa rate  $b$  is given by [22]:

$$b = \left( \frac{1/T_{\text{ceL}}}{1/T_{\text{ceI}} + 1/T_{\text{ceL}}} \right) b_K \quad (3)$$

In the strong bottleneck regime, the exchange scattering will no longer determine the relaxation (at least not in first order), since  $1/T_{\text{ceI}} \propto J^2$ . The expression for  $\Delta H$  is usually casted in the following form [22]:

$$\Delta H = \Delta H_0 + \frac{\chi_e}{\chi_{\text{dc}}} \frac{1}{T_{\text{ceL}}} \quad (4)$$

where  $\chi_e$  is the susceptibility of the itinerant electronic system (usually the Pauli susceptibility), and  $\chi_{\text{dc}}$  is the measured  $dc$ -susceptibility of the local moment. It is noteworthy that Eq. 4 mimics the Korringa relaxation but, in contrast, depends strongly on the concentration of the ESR probe. A similar expression can also be deduced by the general arguments given by Huber [24]. In the following, we shall explain how Eq. 3 and in particular Eq. 4 are more appropriate than Eq. 2 to address the existing experimental data.

We begin discussing Fig. 2, which shows the  $X$ -band and  $Q$ -band linewidth and  $g$ -values (in the inset) for the  $\text{EuFe}_{1.9}\text{Co}_{0.1}\text{As}_2$  sample, which is the only sample investigated displaying a SDW transition. We confirm a linear increase of  $\Delta H$  for  $T > T_N^{\text{SDW}} = 100$  K, and a dome-like behavior of  $\Delta H$  [26] between  $40 \leq T \leq 100$  K (not present in Ref. [21]). The  $g$ -values (see inset) are insensitive to the change in the relaxation regime. Furthermore, the relaxation is slightly slower at  $Q$ -band.

In principle, both expressions (Eqs. 3 and 4) may be used to explain the behavior of  $\Delta H$ . For  $T > T_N^{\text{SDW}}$ , one could consider that the linear increase of  $\Delta H$  originates from a reduced Korringa process or from the inverse of the high temperature  $\chi_{\text{dc}}$ . For  $T < T_N^{\text{SDW}}$ , the dome-like behavior of  $\Delta H$  finds no explanation in the Korringa picture. It could be that it is a coherence peak, due to the gap opening of the SDW transition or, due its sample dependence, it could be ascribed to the dome which is observed in

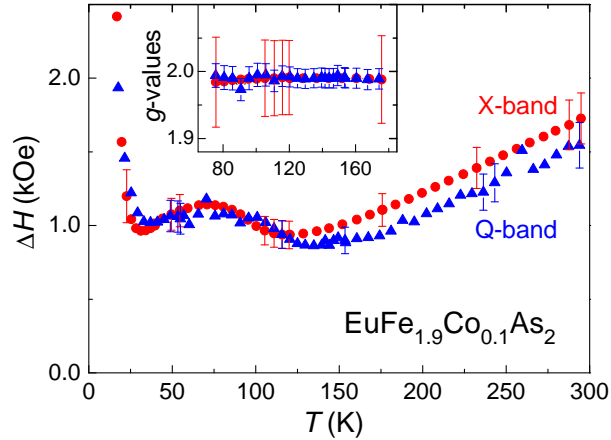


**Figure 2.** (Color online) The evolution of the linewidth ( $\Delta H$ ) as a function of  $T$  obtained for  $\text{EuFe}_{1.9}\text{Co}_{0.1}\text{As}_2$ , which undergoes a SDW transition at  $T_N^{SDW} = 100$  K. At this temperature, in contrast to all other samples,  $\Delta H$  no longer follows a “Korringa-like” behavior (see text). The inset shows in detail that the  $g$ -values, unlike  $\Delta H$ , are unaffected by this transition at 100 K.

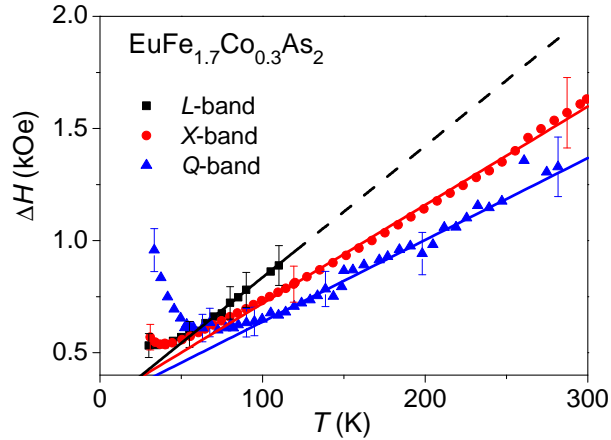


**Figure 3.** (Color online) Temperature dependence of the linewidth ( $\Delta H$ ) of  $\text{EuFe}_{1.7}\text{Co}_{0.3}\text{As}_2$  for  $L$ -band,  $X$ -band, and  $Q$ -band frequencies. The data are representative for all measured, but the  $x = 0.1$ , samples (for  $x = 0.1$  see Fig. 2). The solid lines are the best linear fit to the data taken at  $X$ -band and  $Q$ -band above  $T = 100$  K. The dashed line is an extrapolation of the low temperature fit of  $L$ -band data.

the resistivity [20]. The resistivity is reflected through  $1/T_{\text{ceL}}$ , that comprises all of the scattering processes (energy dissipation) of the itinerant system. The insensitivity of the  $g$ -values to the changes of the relaxation regime indicates a strong relaxation bottleneck.

For all other measured samples (with  $x > 0.1$ ), the evolution of  $\Delta H$ , as a function of temperature and frequency/field, is well represented by the data in Fig. 3, which displays the  $L$ -band,  $X$ -band, and  $Q$ -band linewidth for  $\text{EuFe}_{1.7}\text{Co}_{0.3}\text{As}_2$ . For  $T \geq 40$



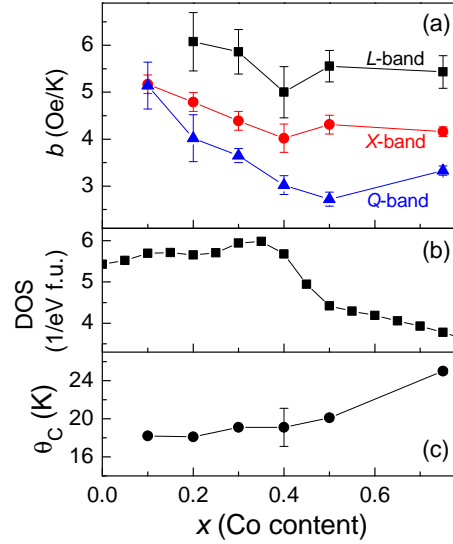


**Figure 4.** (Color online) Evolution as a function of Co-substitution of (a) the  $b$  parameter, obtained at different frequencies/fields, extracted from a linear fitting of  $\Delta H$  as a function of temperature, (b) the calculated total density of states (DOS), and (c) the Curie temperature  $\theta_C$  obtained from dc-susceptibility measurements.

K  $\Delta H$  broadens linearly with increasing temperature whereas in the low temperature region, with decreasing temperature, the proximity of the magnetic phase transition leads to the observed fast broadening of  $\Delta H$ . The linear increase was fitted to the expression  $\Delta H = \Delta H_0 + bT$  for  $80 \text{ K} \leq T \leq 120 \text{ K}$  in the case of the  $L$ -band data and for  $100 \text{ K} \leq T \leq 300 \text{ K}$  in the cases of the  $X$ - and  $Q$ -band data. The dashed line shows an extrapolation for  $T \geq 120 \text{ K}$  of the  $L$ -band fitting result.

The obtained  $b$  parameters are compiled in Fig. 4(a) as a function of frequency/field and Co-substitution. As a function of  $x$ , the  $b$  parameter decreases along the series and is nearly constant for  $x > 0.4$ . With increasing the applied frequency/field the  $b$  parameter is clearly reduced. This is best pronounced in the region  $x \geq 0.2$  where instead of the now fully suppressed ordered phase of the itinerant subsystem, one expects strong magnetic fluctuations.

The observed behavior of the  $b$  parameter on the frequency, being understood as an effect of the frequency-equivalent magnetic field, can be explained by the dependence of the  $b$  parameter on  $1/T_{\text{ceL}}$ . In a magnetic compound, the itinerant subsystem will also dissipate energy through a magnetic process, meaning that  $1/T_{\text{ceL}}$  is also sensitive to spin-spin scattering. A relatively higher field suppresses the magnetic fluctuations in the system thus lowering the scattering rate of the conduction electrons by the magnetic fluctuations (spin-spin scattering). Therefore, as observed [Fig. 4(a)], at higher fields  $b$  should be smaller.

The evolution of the  $b$  parameter as a function of the Co-substitution is a somewhat more evolved subject and a number of distinct effects should be considered. First,

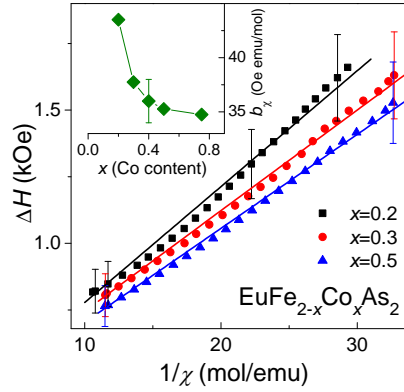


**Figure 5.** (Color online) Plot of  $\Delta H$  as a function of reciprocal susceptibility  $1/\chi_{dc}$  ( $H = 1$  kOe,  $T \geq 100$  K). The solid line is the linear fitting of the data and the obtained coefficient  $b_\chi$  is presented as a function of Co-substitution in the inset.

we consider that the the Co-substitution contributes to the DOS at the Fermi level  $[\eta(E_F)]$  by electronic doping. In the case of a relaxation dominated by the Korringa process,  $b$  should be proportional to  $\eta(E_F)^2$  (see Eq. 2). To further investigate this point, we performed band structure calculations to reveal the change of  $\eta(E_F)$  upon Co-substitution. It has been shown previously that the effect of Co-substitution on the SDW, which is closely related to the Fermi surface, can be well described using the VCA [9]. The result for  $0 < x < 0.8$  is presented in Fig. 4(b).  $\eta(E_F)$  shows a small upwards variation for  $x$  up to  $\approx 0.4$ , and then starts to decrease continuously for higher values of  $x$ . This behavior is nearly opposite to the one observed in  $b$ .

The evolution of the local moment fluctuations, as expressed by the Curie temperature  $\theta_C$ , along the series is presented in Fig. 4(c). Due to the effects of exchange narrowing,  $\Delta H$  would be narrower for larger fluctuations. Accordingly,  $b$  should decrease monotonically as  $\theta_C$  increases. However, this is not the observed behavior, suggesting that the local moment fluctuations alone cannot explain the evolution of the  $\text{Eu}^{2+}$  spin relaxation as function of Co-substitution.

In Fig. 5 we present some relevant information to this discussion. We follow the suggestion of Eq. 4 and show a plot of  $\Delta H$  as function of  $1/\chi_{dc}$ . It is clearly seen that for a broad temperature interval,  $T \geq 100$  K,  $\Delta H$  is proportional to  $1/\chi_{dc}$ . The slopes of these curves ( $b_\chi$ ), for the whole set of samples (but the  $x = 0.1$  sample), are compiled in the inset of the figure. A good qualitative correlation between the concentration dependence of the  $b$  parameter and the results of the slopes  $b_\chi$  is found (see inset of Fig. 5). Following Eq. 4, this slope should be written as  $b_\chi \approx \chi_e(1/T_{ceL})$ , meaning that it expresses an interplay between the magnetism of the itinerant states in the  $\text{Fe}_{2-x}\text{Co}_x\text{As}_2$  layers ( $\chi_e$ ) and the multiple scattering processes taking place in the system ( $1/T_{ceL}$ ).

On a technical level, the above results when put together strongly suggest that the Korringa process has a marginal role in the spin relaxation in these systems. This

means that the  $\text{Eu}^{2+}$  spin relaxation is driven by the indirect RKKY coupling among the  $\text{Eu}^{2+}$  spins, that is under the influence of the magnetic fluctuations of the itinerant subsystem.

The field dependence of the relaxation reveals the presence of strong magnetic fluctuations after the total suppression of the AFM order of the itinerant subsystem. For  $x > 0.4$ , where  $b$  is nearly constant as a function of  $x$ , the field dependence of  $b$  is strongly pronounced, suggesting stronger magnetic fluctuations than for  $x < 0.4$ . Furthermore, the field dependence of the relaxation testifies to the existence of magnetic fluctuations even at relatively high levels of Co-substitution in the  $\text{Fe}_{2-x}\text{Co}_x\text{As}_2$  layers.

As already noted, the suppression of the superconducting state by the pair-breaking effect of the  $\text{Eu}^{2+}$  moments in optimally doped  $\text{Sr}_{1-y}\text{Eu}_y\text{Fe}_{2-x}\text{Co}_x\text{As}_2$  was recently addressed [17] and here we use the data of Ref. [17] in the subsequent discussion. Pair breaking by a paramagnetic impurity in a superconductor is described by the Abrikosov-Gorkov expression and is driven by an effective exchange scattering that was demonstrated to be comparable with those determined by ESR [37] (see Eq. 2). The required DOS for this calculation was shown to be nearly the same for  $\text{SrFe}_2\text{As}_2$  and  $\text{EuFe}_2\text{As}_2$ , and amounts to  $\eta(E_F) = 0.8$  states/eV.f.u. [7]. The estimated exchange scattering is  $J = 6.1$  meV which, by Eq. 2, would drive a relaxation no faster than 1 Oe/K. This should be taken as an upper bound for the value of  $b_K$  if the relaxation were determined by the Korringa process. Therefore, this result provides further evidence for the above described scenario where the relaxation is driven by the exchange coupling among the local spins [24]. In the case of a more traditional bottleneck effect [28, 27, 22], the magnetic fluctuations could increase the apparent relaxation rate by partially, or completely, opening the bottleneck. However, the Korringa rate  $b_K$  could not exceed the value of  $b_K = 1$  Oe/K estimated for a full Korringa process. Although not conclusive, this is another important point in favor of an exchange coupled spins scenario to interpret the bottleneck in  $\text{EuFe}_{2-x}\text{Co}_x\text{As}_2$ .

#### 4. Conclusions

From investigating the field dependence of the  $\text{Eu}^{2+}$  spin resonance in the series  $\text{EuFe}_{2-x}\text{Co}_x\text{As}_2$  we found that the electronic properties of the itinerant subsystem are directly reflected in the ESR relaxation mechanism. We have shown that this is achieved in terms of a so-called relaxation bottleneck of exchange coupled  $\text{Eu}^{2+}$  spins. In particular, this kind of relaxation mechanism is suggested by the opposing evolutions of the linewidth slope ( $b$ ) and the calculated DOS at the Fermi level along the series.

The clear field dependence of the relaxation indicates the presence of magnetic fluctuations and provides a picture of how the relative strength of the itinerant magnetic fluctuations evolves along the series. Interestingly, this field dependence is well pronounced for  $x \geq 0.2$  where the AFM order of the itinerant subsystem is suppressed, indicating it is a property of the emerging itinerant magnetic fluctuations. Furthermore, the field effect is visible even at  $x = 0.75$  which is far away from  $x = 0.2$ .

The ESR results add further evidence that the presence of the  $\text{Eu}^{2+}$  spins nearly does not affect the electronic or magnetic properties of the itinerant subsystem. Therefore, one could expect that our picture on the evolution of the magnetic fluctuations is a general property of the  $\text{Fe}_{2-x}\text{Co}_x\text{As}_2$  layers.

## Acknowledgments

We are in great debt to Deepa Kasinathan for many discussions on the properties of the  $\text{EuFe}_2\text{As}_2$  system. Part of this work has been performed within the framework of DFG SPP1458.

## References

- [1] Kamihara Y, Watanabe T, Hirano M and Hosono H 2008 *J. Am. Chem. Soc.* **130** 3296–3297 ISSN 0002-7863
- [2] Zhi-An R, Wei L, Jie Y, Wei Y, Xiao-Li S, Zheng-Cai, Guang-Can C, Xiao-Li D, Li-Ling S, Fang Z and Zhong-Xian Z 2008 *Chinese Physics Letters* **25** 2215–2216 ISSN 0256-307X, 1741-3540
- [3] Johnston D C 2010 *Advances in Physics* **59** 803–1061 ISSN 00018732
- [4] Monthoux P, Pines D and Lonzarich G G 2007 *Nature* **450** 1177–1183 ISSN 0028-0836
- [5] Saxena S S, Agarwal P, Ahilan K, Grosche F M, Haselwimmer R K W, Steiner M J, Pugh E, Walker I R, Julian S R, Monthoux P, Lonzarich G G, Huxley A, Sheikin I, Braithwaite D and Flouquet J 2000 *Nature* **406** 587–592 ISSN 0028-0836
- [6] Le Tacon M, Ghiringhelli G, Chaloupka J, Sala M M, Hinkov V, Haverkort M W, Minola M, Bakr M, Zhou K J, Blanco-Canosa S, Monney C, Song Y T, Sun G L, Lin C T, De Luca G M, Salluzzo M, Khaliullin G, Schmitt T, Braicovich L and Keimer B 2011 *Nat Phys* **7** 725–730 ISSN 1745-2473
- [7] Jeevan H, Hossain Z, Kasinathan D, Rosner H, Geibel C and Gegenwart P 2008 *Phys. Rev. B* **78** ISSN 1098-0121, 1550-235X
- [8] Ren Z, Zhu Z, Jiang S, Xu X, Tao Q, Wang C, Feng C, Cao G and Xu Z 2008 *Phys. Rev. B* **78** 052501
- [9] Kasinathan D, Ormeci A, Koch K, Burkhardt U, Schnelle W and Rosner H 2009 *New journal of physics* **11** ISSN 1367-2630
- [10] Xiao Y, Su Y, Meven M, Mittal R, Kumar C M N, Chatterji T, Price S, Persson J, Kumar N, Dhar S K, Thamizhavel A and Brueckel T 2009 *Phys. Rev. B* **80** 174424
- [11] Jeevan H S, Hossain Z, Kasinathan D, Rosner H, Geibel C and Gegenwart P 2008 *Phys. Rev. B* **78** 092406
- [12] Ying J J, Wu T, Zheng Q J, He Y, Wu G, Li Q J, Yan Y J, Xie Y L, Liu R H, Wang X F and Chen X H 2010 *Phys. Rev. B* **81** 052503
- [13] Jeevan H, Kasinathan D, Rosner H and Gegenwart P 2011 *Phys. Rev. B* **83** ISSN 1098-0121, 1550-235X
- [14] Ren Z, Tao Q, Jiang S, Feng C, Wang C, Dai J, Cao G and Xu Z 2009 *Phys. Rev. Lett.* **102** ISSN 0031-9007
- [15] Miclea C F, Nicklas M, Jeevan H S, Kasinathan D, Hossain Z, Rosner H, Gegenwart P, Geibel C and Steglich F 2009 *Phys. Rev. B* **79** 212509
- [16] Kurita N, Kimata M, Kodama K, Harada A, Tomita M, Suzuki H S, Matsumoto T, Murata K, Uji S and Terashima T 2011 *Phys. Rev. B* **83** 214513
- [17] Hu R, Budko S, Straszheim W and Canfield P 2011 *Phys. Rev. B* **83** 094520
- [18] Zhou B, Zhang Y, Yang L, Xu M, He C, Chen F, Zhao J, Ou H, Wei J, Xie B, Wu T, Wu G,

- Arita M, Shimada K, Namatame H, Taniguchi M, Chen X H and Feng D L 2010 Phys. Rev. B **81** 155124
- [19] Terashima T, Kurita N, Kikkawa A, Suzuki H S, Matsumoto T, Murata K and Uji S 2010 J. Phys. Soc. Jpn. **79** 103706 ISSN 0031-9015
- [20] Nicklas M, Kumar M, Lengyel E, Schnelle W and Leithe-Jasper A 2011 Journal of Physics: Conference Series vol 273 p 012101
- [21] Dengler E, Deisenhofer J, Krug von Nidda H, Khim S, Kim J S, Kim K H, Casper F, Felser C and Loidl A 2010 Phys. Rev. B **81** ISSN 1098-0121
- [22] Barnes S 1981 Advances in Physics **30** 801–938 ISSN 0001-8732
- [23] Van Vleck J H 1948 Phys. Rev. **74** 1168–1183
- [24] Huber D L 1976 Phys. Rev. B **13** 291–294
- [25] Pascher N, Deisenhofer J, von Nidda H A, Hemmida M, Jeevan H S, Gegenwart P and Loidl A 2010 Arxiv preprint arXiv:1001.1302
- [26] Garcia F A, Bittar E M, Adriano C, Garitezi T M, Rettori C and Pagliuso P G 2011 Journal of Physics: Conference Series **273** 012093 ISSN 1742-6596
- [27] Rettori C, Kim H M, Chock E P and Davidov D 1974 Phys. Rev. B **10** 1826
- [28] Rettori C, Davidov D, Orbach R, Chock E P and Ricks B 1973 Phys. Rev. B **7** 1
- [29] Joshi J P and Bhat S V 2004 J. Magn. Reson. **168** 284–287 ISSN 1090-7807
- [30] Wykhoff J, Sichelschmidt J, Lapertot G, Knebel G, Flouquet J, Fazlishanov I I, Krug von Nidda H, Krellner C, Geibel C and Steglich F 2007 Science and Technology of Advanced Materials **8** 389–392 ISSN 1468-6996
- [31] Opahle I, Koepf K and Eschrig H 1999 Phys. Rev. B **60** 14035–14041
- [32] Perdew J P and Wang Y 1992 Phys. Rev. B **45** 13244–13249
- [33] Kasinathan D, Wagner M, Koepf K, Cardoso-Gil R, Grin Y and Rosner H 2012 Phys. Rev. B **85** 035207
- [34] Uhoya W, Tsoi G, Vohra Y K, McGuire M A, Sefat A S, Sales B C, Mandrus D and Weir S T 2010 J. Phys.: Condens. Matter **22** 292202 ISSN 0953-8984, 1361-648X
- [35] Rotter M, Hieke C and Johrendt D 2010 Phys. Rev. B **82** 014513
- [36] Chen X, Ren Z, Ding H and Liu L 2010 SCIENCE CHINA Physics, Mechanics & Astronomy **53** 1212–1215
- [37] Davidov D, Chelkowski A, Rettori C, Orbach R and Maple M B 1973 Phys. Rev. B **7** 1029